New relativistic mean-field interaction with density-dependent meson-nucleon couplings

Lalazissis, G. A.; Nikšić, Tamara; Vretenar, Dario; Ring, Peter

New relativistic mean-field interaction with density-dependent meson-nucleon couplings

G. A. Lalazissis
Department of Theoretical Physics, Aristotle University of Thessaloniki, GR-54124, Greece and Physik-Department der Technischen Universität München, D-85748 Garching, Germany

T. Nikšić and D. Vretenar
Physics Department, Faculty of Science, University of Zagreb, Croatia and Physik-Department der Technischen Universität München, D-85748 Garching, Germany

P. Ring
Physik-Department der Technischen Universität München, D-85748 Garching, Germany

(Received 21 July 2004; published 25 February 2005)

We adjust a new improved relativistic mean-field effective interaction with explicit density dependence of the meson-nucleon couplings. The effective interaction DD-ME2 is tested in relativistic Hartree-Bogoliubov and quasiparticle random-phase approximation (QRPA) calculations of nuclear ground states and properties of excited states, in calculation of masses, and it is applied to the analysis of very recent data on superheavy nuclei.

DOI: 10.1103/PhysRevC.71.024312 PACS number(s): 21.60.−n, 21.30.Fe, 21.65.+f, 21.10.−k

I. INTRODUCTION

Structure properties of medium-heavy and heavy nuclei with many active valence nucleons are best described in the framework of self-consistent mean-field methods. The effective Gogny interaction, the Skyrme energy functionals, and the relativistic meson-exchange effective Lagrangians have been very successfully employed in models of nuclear structure and low-energy dynamics [1].

The self-consistent mean-field approach enables a description of the nuclear many-body problem in terms of a universal energy density functional. The exact energy functional, which includes all higher order correlations, is approximated with powers and gradients of ground-state nucleon densities. Although it models the effective interaction between nucleons, a general density functional is not necessarily related to any given *NN* potential. By employing global effective interactions, adjusted to empirical properties of symmetric and asymmetric nuclear matter, and to bulk properties of few spherical nuclei, self-consistent mean-field models have achieved a high level of accuracy in the description of ground states and properties of excited states in arbitrarily heavy nuclei. One of the major goals of modern nuclear structure is to build a universal energy density functional theory [2]. The theory is universal in the sense that the same functional is used for all nuclei, with the same set of parameters. This framework should provide a basis for a consistent microscopic treatment of the nuclear many-body problem, including infinite nuclear and neutron matter, ground-state properties of all bound nuclei, low-energy excited states, small-amplitude vibrations, large-amplitude adiabatic properties, and reliable extrapolations toward the drip lines.

One of the first steps in this direction has been the construction of microscopic mass tables based on the self-consistent Skyrme Hartree-Fock (HF) and Skyrme Hartree-Fock-Bogoliubov (HFB) framework. In a series of recent papers [3–6] a set of complete microscopic mass tables of more than 9000 nuclei lying between the particle drip lines over the range $Z, N \geqslant 8$ and $Z \leqslant 120$ have been constructed within the HFB framework. By adjusting the parameters of the Skyrme interaction, the strength and the cutoff parameters of the (possibly density-dependent) δ-function pairing force, and the parameters of two phenomenological Wigner terms, with a total of $\approx$20 parameters in all, the measured masses of 2135 nuclei with $Z, N \geqslant 8$ have been fitted with an rms error of less than 700 keV. In addition, although these effective interactions have been adjusted only to masses, they also produce excellent results for the charge radii, with an rms deviation of $\approx$0.025 fm for the absolute charge radii and charge isotope shifts of more than 500 nuclei [7]. However, the Skyrme-HFB mass formulas are far from being definite. Future improvements must include modifications to the interactions, a better treatment of symmetry-breaking effects, and many-body correlations. For instance, in Ref. [8] an improved version of the deformed configuration-space HFB method has been employed, based on the expansion of the HFB wave functions in a complete set of transformed harmonic-oscillator basis states, obtained by a local-scaling point transformation. This method enables a careful treatment of the asymptotic part of the nucleonic density and is therefore particularly suitable for self-consistent HFB calculations of deformed weakly bound nuclei close to the nucleon drip lines. In Ref. [9] the coordinate-space HFB framework has been generalized to include arbitrary mixing between protons and neutrons both in the particle-hole and particle-particle channels. The resulting HFB density matrices have a rich spin-isospin structure and provide a microscopic description of pairing correlations in all isospin channels.

An important class of self-consistent mean-field models belongs to the framework of relativistic mean-field theory (RMF). RMF-based models have been successfully applied in analyses of a variety of nuclear structure phenomena, not only in nuclei along the valley of β stability, but also

in exotic nuclei with extreme isospin values and close to the particle drip lines. The RMF framework has recently been extended to include effective Lagrangians with density-dependent meson-nucleon vertex functions. The functional form of the meson-nucleon vertices can be deduced from in-medium Dirac-Brueckner interactions, obtained from realistic free-space *NN* interactions, or a phenomenological approach can be adopted, with the density dependence for the σ, ω, and ρ meson-nucleon couplings adjusted to properties of nuclear matter and a set of spherical nuclei. The latter was employed in Ref. [10], where the relativistic Hartree-Bogoliubov (RHB) model was extended to include medium-dependent vertex functions. It has been shown that, in comparison with standard nonlinear meson self-interactions, relativistic models with an explicit density dependence of the meson-nucleon couplings provide an improved description of asymmetric nuclear matter, neutron matter, and nuclei far from stability. The relativistic random-phase approximation (RRPA), based on effective Lagrangians characterized by density-dependent meson-nucleon vertex functions, has been derived in Ref. [11]. A comparison of the RRPA results on multipole giant resonances with experimental data provides additional constrains on the parameters that characterize the isoscalar and isovector channels of the density-dependent effective interactions. In a microscopic analysis of the nuclear matter compressibility and symmetry energy [12], it has been shown that the experimental data on the giant monopole resonances restrict the nuclear matter compression modulus of structure models based on the relativistic mean-field approximation to $K_{\rm nm} \approx 250$–270 MeV, whereas the isovector giant dipole resonances and the available data on differences between neutron and proton radii limit the range of the nuclear matter symmetry energy at saturation (volume asymmetry) of these effective interactions to $32\,\text{MeV} \leqslant a_4 \leqslant 36\,\text{MeV}$.

In this work we continue the investigation of relativistic effective forces with density-dependent meson-nucleon couplings, and we adjust a new phenomenological interaction to be used in RMF+BCS, RHB, and relativistic quasiparticle random-phase approximation [R(Q)RPA] calculations of ground states and excitations of spherical and deformed nuclei. The construction of the effective interaction DD-ME2 and the resulting equations of state for symmetric and asymmetric nuclear matter are analyzed in Sec. II. In Sec. III the new interaction is employed in a series of RHB and R(Q)RPA calculations of ground-state properties and giant resonances. The model is tested in the calculation of masses and is applied to the analysis of very recent data on superheavy nuclei. The results are summarized in Sec. IV.

II. THE EFFECTIVE DENSITY-DEPENDENT INTERACTION DD-ME2

References [13–15] contain a very detailed discussion of the density-dependent nuclear hadron field theory. The relativistic RHB model and the random phase approximation (RPA) based on effective interactions with density-dependent meson-nucleon couplings are described in Refs. [10] and [11], respectively. For completeness we include the essential features of the relativistic Lagrangian density with medium-dependent vertices

$$\begin{aligned}\mathcal{L} = {} & \bar{\psi}\left(i\gamma\cdot\partial - m\right)\psi + \frac{1}{2}(\partial\sigma)^2 - \frac{1}{2}m_\sigma\sigma^2 - \frac{1}{4}\Omega_{\mu\nu}\Omega^{\mu\nu} \\ & + \frac{1}{2}m_\omega^2\omega^2 - \frac{1}{4}\vec{R}_{\mu\nu}\vec{R}^{\mu\nu} + \frac{1}{2}m_\rho^2\vec{\rho}^{\,2} - \frac{1}{4}F_{\mu\nu}F^{\mu\nu} - g_\sigma\bar{\psi}\sigma\psi \\ & - g_\omega\bar{\psi}\gamma\cdot\omega\psi - g_\rho\bar{\psi}\gamma\cdot\vec{\rho}\vec{\tau}\psi - e\bar{\psi}\gamma\cdot A\frac{(1-\tau_3)}{2}\psi. \end{aligned} \tag{1}$$

Vectors in isospin space are denoted by arrows, and bold-faced symbols will indicate vectors in ordinary three-dimensional space. The Dirac spinor ψ denotes the nucleon with mass m. The masses m_σ, m_ω, and m_ρ are those of the σ meson, the ω meson, and the ρ meson, with g_σ, g_ω, and g_ρ being the corresponding coupling constants for the mesons to the nucleon. This Lagrangian is, of course, invariant under parity transformation and, since we only consider solutions with well-defined parity, the expectation value of the pseudoscalar pion field vanishes in the Hartree approximation. The coupling constants and unknown meson masses are parameters, adjusted to reproduce nuclear matter properties and ground-state properties of finite nuclei. Here $\Omega^{\mu\nu}$, $\vec{R}^{\mu\nu}$, and $F^{\mu\nu}$ are the field tensors of the vector fields ω, ρ, and of the photon:

$$\Omega^{\mu\nu} = \partial^\mu\omega^\nu - \partial^\nu\omega^\mu, \tag{2}$$

$$\vec{R}^{\mu\nu} = \partial^\mu\vec{\rho}^{\,\nu} - \partial^\nu\vec{\rho}^{\,\mu}, \tag{3}$$

$$F^{\mu\nu} = \partial^\mu A^\nu - \partial^\nu A^\mu. \tag{4}$$

The functions g_σ, g_ω, and g_ρ are assumed to be vertex functions of Lorentz-scalar bilinear forms of the nucleon operators. In practical applications of the density-dependent hadron field theory the meson-nucleon couplings are assumed to be functions of the baryon density $\psi^\dagger\psi$. In a relativistic framework the couplings can also depend on the scalar density $\bar{\psi}\psi$. Nevertheless, expanding in $\psi^\dagger\psi$ is the natural choice, because the baryon density is connected to the conserved baryon number, unlike the scalar density for which no conservation law exists. The scalar density is a dynamical quantity, to be determined self-consistently by the equations of motion, and is expandable in powers of the Fermi momentum. For the meson-exchange models it has been shown that the dependence on baryon density alone provides a more direct relation between the self-energies of the density-dependent hadron field theory and the Dirac-Brueckner microscopic self-energies [13]. The explicit dependence of the vertex functions on the baryon density produces rearrangement contributions to the vector nucleon self-energy. The rearrangement terms result from the variation of the vertex functionals with respect to the baryon fields in the density operator (which coincides with the baryon density in the nuclear matter rest frame). For a model with density-dependent couplings, the inclusion of the rearrangement self-energies is essential for energy-momentum conservation and thermodynamical consistency (i.e., for the pressure equation derived from the thermodynamic definition and from the energy-momentum tensor) [14,15].

The meson-nucleon vertex functions are determined either by mapping the nuclear matter Dirac-Brueckner nucleon

self-energies in the local density approximation [13,15,16] or by adjusting the parameters of an assumed phenomenological density dependence of the meson-nucleon couplings to reproduce properties of symmetric and asymmetric nuclear matter and finite nuclei [10,14]. In the phenomenological approach of Refs. [10,13,14] the coupling of the σ meson and ω meson to the nucleon field reads

$$g_i(\rho) = g_i(\rho_{\rm sat}) f_i(x) \quad \text{for} \quad i = \sigma, \omega, \tag{5}$$

where

$$f_i(x) = a_i \frac{1 + b_i(x + d_i)^2}{1 + c_i(x + d_i)^2} \tag{6}$$

is a function of $x = \rho/\rho_{\rm sat}$, and $\rho_{\rm sat}$ denotes the baryon density at saturation in symmetric nuclear matter. The eight real parameters in (6) are not independent. The five constraints—$f_i(1) = 1$, $f''_\sigma(1) = f''_\omega(1)$, and $f''_i(0) = 0$—reduce the number of independent parameters to three. Three additional parameters in the isoscalar channel are $g_\sigma(\rho_{\rm sat})$, $g_\omega(\rho_{\rm sat})$, and m_σ, the mass of the phenomenological σ meson. For the ρ-meson coupling the functional form of the density dependence is suggested by Dirac-Brueckner calculations of asymmetric nuclear matter [16]:

$$g_\rho(\rho) = g_\rho(\rho_{\rm sat}) \exp[-a_\rho(x - 1)]. \tag{7}$$

The isovector channel is parametrized by $g_\rho(\rho_{\rm sat})$ and a_ρ. Usually the free values are used for the masses of the ω and ρ mesons: $m_\omega = 783\,{\rm MeV}$ and $m_\rho = 763\,{\rm MeV}$. In principle one could also consider the density dependence of the meson masses. However, since the effective meson-nucleon coupling in nuclear matter is determined by the ratio g/m, the choice of a phenomenological density dependence of the couplings makes an explicit density dependence of the masses redundant.

The eight independent parameters (seven coupling parameters and the mass of the σ meson) are adjusted to reproduce the properties of symmetric and asymmetric nuclear matter, binding energies, charge radii, and neutron radii of spherical nuclei. In Ref. [10] we introduced the density-dependent meson-exchange effective interaction (DD-ME1), whose parameters are displayed in Table I. The seven coupling parameters and the σ-meson mass were simultaneously adjusted to properties of symmetric and asymmetric nuclear matter, and to ground-state properties of twelve spherical nuclei [17–19]. For the open-shell nuclei pairing correlations were treated in the BCS approximation with empirical pairing gaps (five-point formula).

In Ref. [10] the RHB model with the density-dependent interaction DD-ME1 in the *ph* channel, and with the finite-range Gogny interaction D1S [20] in the *pp* channel, was tested in the analysis of ground-state properties of the Sn and Pb isotopic chains. It has been shown that, compared to standard nonlinear relativistic mean-field effective forces, the interaction DD-ME1 has better isovector properties and therefore provides an improved description of asymmetric nuclear matter, neutron matter, and nuclei far from stability. The DD-ME1 interaction has also recently been tested in the calculation of deformed nuclei [21]. Ground-state properties of six isotopic chains ($60 \leqslant Z \leqslant 70$) in the region of rare-earth nuclei were calculated by using the RHB model, and a very good agreement was obtained in comparison with experimental data on total binding energies, charge isotope shifts, and quadrupole deformation parameters.

TABLE I. The parameters of the effective interactions DD-ME2 and DD-ME1. See text for description.

	DD-ME2	DD-ME1
m_σ	550.1238	549.5255
m_ω	783.0000	783.0000
m_ρ	763.0000	763.0000
$g_\sigma(\rho_{\rm sat})$	10.5396	10.4434
$g_\omega(\rho_{\rm sat})$	13.0189	12.8939
$g_\rho(\rho_{\rm sat})$	3.6836	3.8053
a_σ	1.3881	1.3854
b_σ	1.0943	0.9781
c_σ	1.7057	1.5342
d_σ	0.4421	0.4661
a_ω	1.3892	1.3879
b_ω	0.9240	0.8525
c_ω	1.4620	1.3566
d_ω	0.4775	0.4957
a_ρ	0.5647	0.5008

In Refs. [11,12] we derived the relativistic (quasiparticle) random phase approximation based on effective interactions with density-dependent meson-nucleon couplings. The explicit density dependence of the vertex functions introduces rearrangement terms in the residual two-body interaction. Illustrative calculations were performed for the isoscalar monopole, isovector dipole, and isoscalar quadrupole response of spherical nuclei. Starting from DD-ME1, and by constructing families of interactions with some given characteristic (compressibility, symmetry energy, and effective mass), it has been shown how the comparison of the R(Q)RPA results on multipole giant resonances with experimental data can be used to constrain the parameters that characterize the isoscalar and isovector channel of the density-dependent effective interactions. In particular, in Ref. [12] we have shown that the comparison of the calculated excitation energies with the experimental data on the giant monopole resonances restricts the nuclear matter compression modulus to $K_{\rm nm} \approx 250$–$270\,{\rm MeV}$. To reproduce the isovector giant dipole resonance in ^{208}Pb and the available data on differences between neutron and proton radii, the range of the nuclear matter symmetry energy at saturation (volume asymmetry) is $32\,{\rm MeV} \leqslant a_4 \leqslant 36\,{\rm MeV}$. Very recently [22] DD-ME1 has also been employed in the proton-neutron R(Q)RPA analysis of charge-exchange modes, specifically isobaric analog resonances and Gamow-Teller resonances in spherical nuclei.

Taking into account all these results, in this work we adjust a new phenomenological density-dependent interaction to be used in RMF+BCS, RHB, and R(Q)RPA calculations of ground states and excitations of spherical and deformed nuclei. Similar to the procedure used in Ref. [10] to adjust the interaction DD-ME1, the seven independent coupling parameters and the mass of the σ-meson are adjusted simultaneously to properties of nuclear matter and to binding

TABLE II. The total binding energies BE, charge radii r_c, and the differences between the radii of neutron and proton density distributions $r_{np} = (r_n - r_p)$, used to adjust the interaction DD-ME2. The calculated values are compared with experimental data (values in parentheses). In the last three columns the corresponding deviations dE, dr_c, and dr_{np} (all in %) are included.

Nucleus	BE (MeV)	r_c (fm)	$r_n - r_p$ (fm)	dE	dr_c	dr_{np}
^{16}O	127.801 (127.619)	2.727 (2.730)	−0.03	0.1	−0.1	
^{40}Ca	342.741 (342.052)	3.464 (3.485)	−0.05	0.2	−0.6	
^{48}Ca	414.770 (415.991)	3.481 (3.484)	0.18	−0.3	−0.1	
^{72}Ni	612.655 (613.173)	3.914	0.28	−0.1		
^{90}Zr	783.155 (783.893)	4.275 (4.272)	0.07	−0.1	0.1	
^{116}Sn	986.928 (988.681)	4.615 (4.626)	0.12 (0.12)	−0.2	−0.2	3.8
^{124}Sn	1048.859 (1049.962)	4.671 (4.674)	0.21 (0.19)	−0.1	−0.1	10.7
^{132}Sn	1103.469 (1102.860)	4.718	0.26	0.1		
^{204}Pb	1608.506 (1607.520)	5.500 (5.486)	0.17	0.1	0.3	
^{208}Pb	1638.426 (1636.446)	5.518 (5.505)	0.19 (0.20)	0.1	0.2	−4.7
^{214}Pb	1661.182 (1663.298)	5.568 (5.562)	0.24	−0.1	0.1	
^{210}Po	1649.695 (1645.228)	5.552	0.17	0.3		

energies, charge radii, and differences between neutron and proton radii of spherical nuclei (see Table II). For nuclear matter the "empirical" input is as follows: $E/A = -16$ MeV (5%), $\rho_0 = 0.153$ fm^{-3} (10%), $K_0 = 250$ MeV (10%), and $J = 33$ MeV (10%). The values in parentheses correspond to the error bars used in the fitting procedure. The binding energies of finite nuclei and the charge radii are taken within an accuracy of 0.1% and 0.2%, respectively. Because of the larger experimental uncertainties, the error bar used for the neutron skin is 5%. For the open-shell nuclei pairing correlations are treated in the BCS approximation with empirical pairing gaps (five-point formula). After the solution of the self-consistent equations, the microscopic estimate for the center-of-mass correction is subtracted from the total binding energy,

$$E_{\rm cm} = -\frac{\langle P_{\rm cm}^2 \rangle}{2Am}, \tag{8}$$

where $P_{\rm cm}$ is the total momentum of a nucleus with A nucleons. As in the case of DD-ME1, a set of twelve spherical nuclei is used to adjust the effective interaction. The only difference is that ^{112}Sn has been replaced by ^{72}Ni. In this way a more balanced mass distribution is used in the fit. Much more important, however, is the fact that for the new interaction we have also used data on excitation energies of isoscalar monopole (ISGMR) and isovector dipole giant resonances (IVGDR) in spherical nuclei. The interaction has been adjusted to the excitation energies of the ISGMR and IVGDR in ^{208}Pb, which practically do not display any fragmentation, and it also reproduces in detail the evolution of the IVGDR in the sequence of Sn isotopes. These results will be discussed in the next section.

The parameters of the new interaction, denoted DD-ME2, are listed in Table I, together with the older parameterization DD-ME1. The DD-ME2 results for the binding energies, charge radii, and differences between radii of neutron and proton density distributions for the set of 12 spherical nuclei are compared with experimental data in Table II. The agreement between the calculated values and data is indeed very good. Even though the two parameter sets are rather similar, the χ^2 for the data set of Table II has been considerably improved with the new interaction: $\chi^2 = 55$ for DD-ME2, whereas $\chi^2 = 77$ for DD-ME1. The two interactions display very similar equations of state for symmetric nuclear matter, the symmetry energies as function of the nucleon density, and the neutron matter equations of state (see the corresponding figures in Ref. [10]). The differences are small and thus in Table III we only compare the nuclear matter properties at saturation density, that is, binding energy per nucleon, saturation density, nuclear matter compression modulus, Dirac effective mass, and symmetry energy at saturation. We notice that for DD-ME2 the nuclear matter incompressibility and the symmetry energy at saturation correspond to the lower limits of the allowed values determined by the R(Q)RPA analysis of the isoscalar monopole and isovector dipole giant resonances in heavy spherical nuclei.

III. APPLICATIONS

We have performed several tests of the new interaction in a series of RHB and R(Q)RPA calculations of binding energies, separation energies, charge isotope shifts, deformations, and

TABLE III. Nuclear matter properties at saturation calculated with the density-dependent effective interactions DD-ME2 and DD-ME1.

	DD-ME2	DD-ME1
$\rho_{\rm sat}$ (fm^{-3})	0.152	0.152
E/A (MeV)	−16.14	−16.20
K_0 (MeV)	250.89	244.5
m^*	0.572	0.578
a_4 (MeV)	32.3	33.1

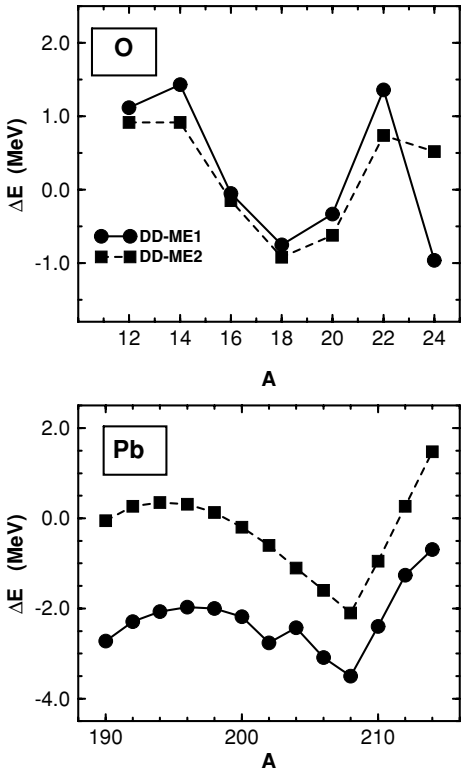

FIG. 1. Differences between the calculated and experimental binding energies for the O and Pb isotopic chains. The theoretical values are calculated in the RHB model with the DD-ME1 and DD-ME2 mean-field effective interactions, and with Gogny pairing.

isoscalar and isovector giant resonances. Ground-state properties have been calculated in the RHB model with the DD-ME2 effective interaction in the particle-hole channel, and with the Gogny interaction [23] in the pairing channel

$$V^{pp}(1,2) = \sum_{i=1,2} e^{-((\mathbf{r}_1-\mathbf{r}_2)/\mu_i)^2} (W_i + B_i P^\sigma - H_i P^\tau - M_i P^\sigma P^\tau), \quad (9)$$

with the set D1S [20] for the parameters μ_i, W_i, B_i, H_i, and M_i $(i = 1, 2)$.

The fully self-consistent RRPA [11] and R(Q)RPA [24] have been used to calculate excitation energies of giant resonances in doubly closed and open-shell nuclei, respectively. The R(Q)RPA is formulated in the canonical basis of the RHB model and, in both the *ph* and *pp* channels, the same interactions are used in the RHB equations that determine the canonical quasiparticle basis and in the matrix equations of the R(Q)RPA.

In general, when compared with the results obtained with the DD-ME1 interaction [10,11,21], the new interaction improves the agreement with experimental data on ground-state properties of spherical and deformed nuclei and excitation energies of giant resonances in spherical nuclei. For instance, in Fig. 1 we display the absolute deviations of the theoretical masses from the experimental values [17]

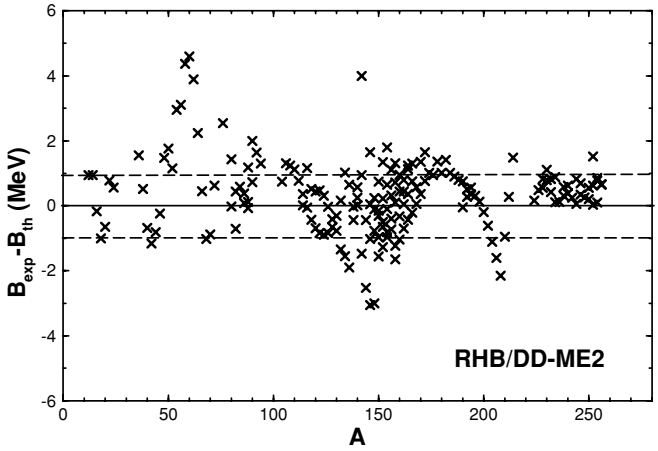

FIG. 2. Absolute deviations of the binding energies calculated with the DD-ME2 interaction from the experimental values [17].

for the isotopic chains of O and Pb. For the O isotopes the absolute deviations calculated with DD-ME1 and DD-ME2 are comparable, generally within $\approx$1 MeV of the experimental data. For the Pb chain, in contrast, the binding energies calculated with the DD-ME2 interaction are in much better agreement with data. However, we are not going to present here a comparison with all the results that were extensively discussed in Refs. [10,11,21] for the DD-ME1 interaction. Rather, selected features of the DD-ME2 interaction will be illustrated.

The theoretical binding energies of approximately 200 nuclei calculated in the RHB model, with the DD-ME2 plus Gogny D1S interactions, are compared with experimental values in Fig. 2. Except for a few Ni isotopes with $N \approx Z$ that are notoriously difficult to describe in a pure mean-field approach, and several transitional medium-heavy nuclei, the calculated binding energies are generally in very good agreement with experimental data. Although this illustrative calculation cannot be compared with microscopic mass tables that include more than 9000 nuclei [3–6], we emphasize that the rms error including all the masses shown in Fig. 2 is less than 900 keV. Moreover, since a finite-range pairing interaction is used, the results are insensitive to unphysical parameters like, for instance, the momentum cutoff in the pairing channel. When compared with data on absolute charge radii and charge isotope shifts from Ref. [19], the calculated charge radii exhibit an rms error of only 0.017 fm. The predictive power of the RHB model with the DD-ME2 effective interaction is also illustrated in Table IV, where we include the calculated binding energies, radii of charge and neutron density distributions, and quadrupole and hexadecupole moments of heavy and superheavy nuclei, in comparison with available experimental data [17–19,25]. The calculated masses and moments are in excellent agreement with experimental values. The results shown in Fig. 2 and Table IV indicate that DD-ME2 could be used as a basis for a microscopic mass table based on a relativistic universal energy density functional. Work along these lines is in progress.

TABLE IV. RHB model (DD-ME2 plus Gogny D1S pairing) results for the binding energies, radii of charge and neutron density distributions, and quadrupole and hexadecupole moments of heavy and superheavy nuclei, in comparison with experimental data [17–19,25].

Nucleus	*BE* (MeV)	r_c (fm)	r_n (fm)	Q_p (b)	H_p (b^2)
^{224}Ra	1720.47 (1720.31)	5.71	5.85	4.93 (6.33)	0.45
^{226}Ra	1731.13 (1731.61)	5.74	5.88	6.22 (7.19)	0.65
^{228}Ra	1741.67 (1742.49)	5.76	5.92	7.44 (7.76)	0.79
^{230}Ra	1751.94 (1753.05)	5.79	5.95	8.39	0.86
^{228}Th	1743.04 (1742.49)	5.78	5.90	7.64 (8.42)	0.88
^{230}Th	1751.94 (1753.05)	5.80	5.93	8.57 (8.99)	0.97 (1.09)
^{232}Th	1766.10 (1766.92)	5.82	5.96	9.28 (9.66)	1.00 (1.22)
^{234}Th	1776.80 (1777.68)	5.84	5.99	9.78 (8.96)	0.96
^{232}U	1766.39 (1765.97)	5.83	5.94	9.57 (10.00)	1.10
^{234}U	1778.66 (1778.57)	5.85	5.97	10.10 (10.35)	1.10 (1.40)
^{236}U	1790.29 (1790.42)	5.87	6.00	10.46 (10.80)	1.03 (1.30)
^{238}U	1801.38 (1801.69)	5.88	6.02	10.74 (11.02)	0.94 (0.83)
^{240}U	1811.82 (1812.44)	5.90	6.05	11.03	0.86
^{238}Pu	1801.85 (1801.27)	5.89	6.01	11.09 (11.26)	1.00 (1.38)
^{240}Pu	1813.84 (1813.46)	5.91	6.03	11.32 (11.44)	1.00 (1.15)
^{242}Pu	1825.26 (1825.01)	5.92	6.05	11.55 (11.61)	0.90
^{244}Pu	1836.00 (1836.06)	5.94	6.08	11.61 (11.73)	0.79
^{246}Pu	1845.97 (1846.66)	5.95	6.10	11.52 (11.52)	0.66
^{244}Cm	1836.67 (1835.85)	5.95	6.06	12.03 (12.14)	0.91
^{246}Cm	1848.17 (1847.83)	5.96	6.08	12.08 (12.26)	0.80
^{248}Cm	1858.94 (1859.20)	5.97	6.11	12.01 (12.28)	0.67
^{250}Cm	1869.20 (1869.75)	5.98	6.13	11.81	0.54
^{250}Cf	1870.20 (1870.00)	6.00	6.11	12.41 (12.70)	0.62
^{252}Cf	1881.31 (1881.28)	6.01	6.13	12.22 (12.95)	0.49
^{254}Cf	1892.02 (1892.12)	6.02	6.15	11.97	0.36
^{252}Fm	1879.55 (1878.93)	6.02	6.12	12.86	0.57
^{254}Fm	1891.85 (1890.99)	6.03	6.14	12.58	0.41
^{256}Fm	1903.21 (1902.55)	6.04	6.16	12.45	0.31
^{252}No	1872.83 (1871.31)	6.03	6.10	13.23	0.56
^{254}No	1886.39 (1885.61)	6.04	6.12	13.22	0.45
^{256}No	1899.21 (1898.65)	6.05	6.15	13.05	0.34
^{256}Rf	1892.38 (1890.67)	6.07	6.13	13.57	0.34
^{260}Sg	1910.95 (1909.05)	6.10	6.16	13.70	0.15
^{264}Hs	1929.96 (1926.75)	6.13	6.18	13.42	−0.05

In adjusting the parameters of DD-ME2 we took into account the results of Refs. [11,12], where it has been shown that, to reproduce the excitation energies of the ISGMR and IVGDR in spherical nuclei, the values of the nuclear matter compression modulus $K_{\rm nm}$ should be restricted to the interval ≈250–270 MeV, and the range of the nuclear matter symmetry energy at saturation should be $32\,{\rm MeV} \leqslant a_4 \leqslant 36\,{\rm MeV}$. For ^{208}Pb the RRPA results for the monopole and isovector dipole response are displayed in Fig. 3. For the multipole operator $\hat{Q}_{\lambda\mu}$ the response function $R(E)$ is defined as

$$R(E) = \sum_i B(\lambda_i \rightarrow 0_f) \frac{\Gamma/2\pi}{(E - E_i)^2 + \Gamma^2/4}, \qquad (10)$$

where Γ is the width of the Lorentzian distribution, and

$$B(\lambda_i \rightarrow 0_f) = \frac{1}{2J+1} |\langle 0_f || \hat{Q}_\lambda || \lambda_i \rangle|^2. \qquad (11)$$

In the examples considered here, the continuous strength distributions are obtained by folding the discrete spectrum of R(Q)RPA states with the Lorentzian [see Eq. (10)] with constant width $\Gamma = 1\,{\rm MeV}$. The calculated peak energies of the ISGMR and IVGDR, 13.9 and 13.5 MeV, respectively, should be compared with the experimental excitation energies, $E = 14.1 \pm 0.3\,{\rm MeV}$ [26] for the monopole resonance and $E = 13.3 \pm 0.1\,{\rm MeV}$ [27] for the dipole resonance, respectively.

In Fig. 4 we compare the R(Q)RPA results for the Sn isotopes with experimental data on IVGDR excitation energies [28]. In contrast to the case of ^{208}Pb, the strength distributions in the region of giant resonances exhibit fragmentation and the energy of the resonance $E_{\rm GDR}$ is defined as the centroid energy $\bar{E} = m_1/m_0$, calculated in the same energy window as the one used in the experimental analysis (13–18 MeV). The RHB+R(Q)RPA calculation with the DD-ME2 interaction reproduces in detail the experimental excitation energies and the isotopic dependence of the IVGDR.

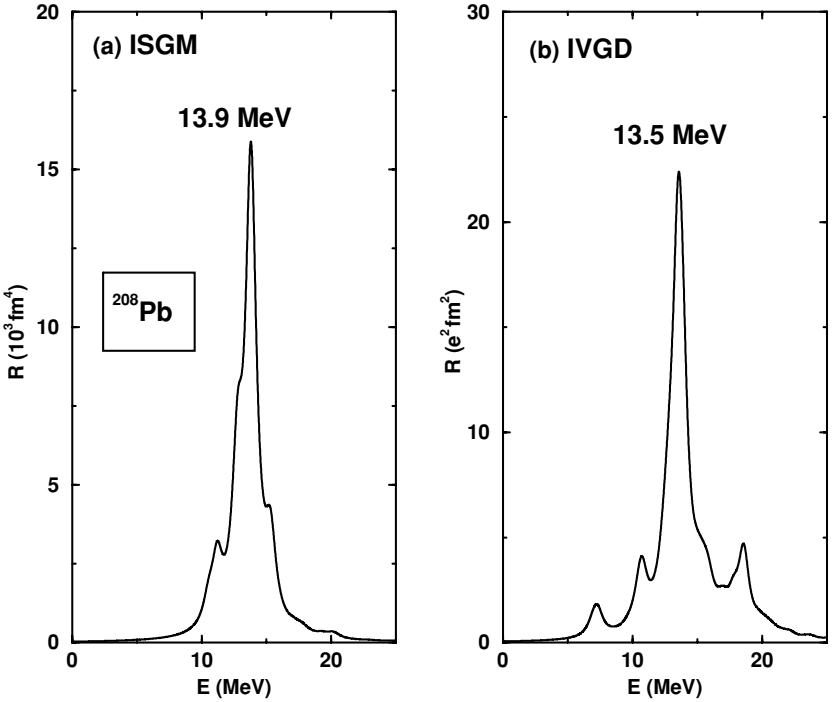

FIG. 3. The isoscalar monopole (a), and the isovector dipole (b) strength distributions in ^{208}Pb calculated with the effective interaction DD-ME2. The experimental excitation energies are 14.1 ± 0.3 MeV [26] for the monopole resonance and 13.3 ± 0.1 MeV [27] for the dipole resonance, respectively.

An important field of applications of self-consistent mean-field models includes the structure and decay properties of superheavy nuclei [1]. The relativistic mean-field framework has recently been very successfully employed in calculations of chains of superheavy isotopes [29–38]. Because generally relativistic density-dependent effective interactions provide a very realistic description of asymmetric nuclear matter, neutron matter, and nuclei far from stability, one can also expect a good description of the structure of superheavy nuclei. In Table IV we have shown that the interaction DD-ME2

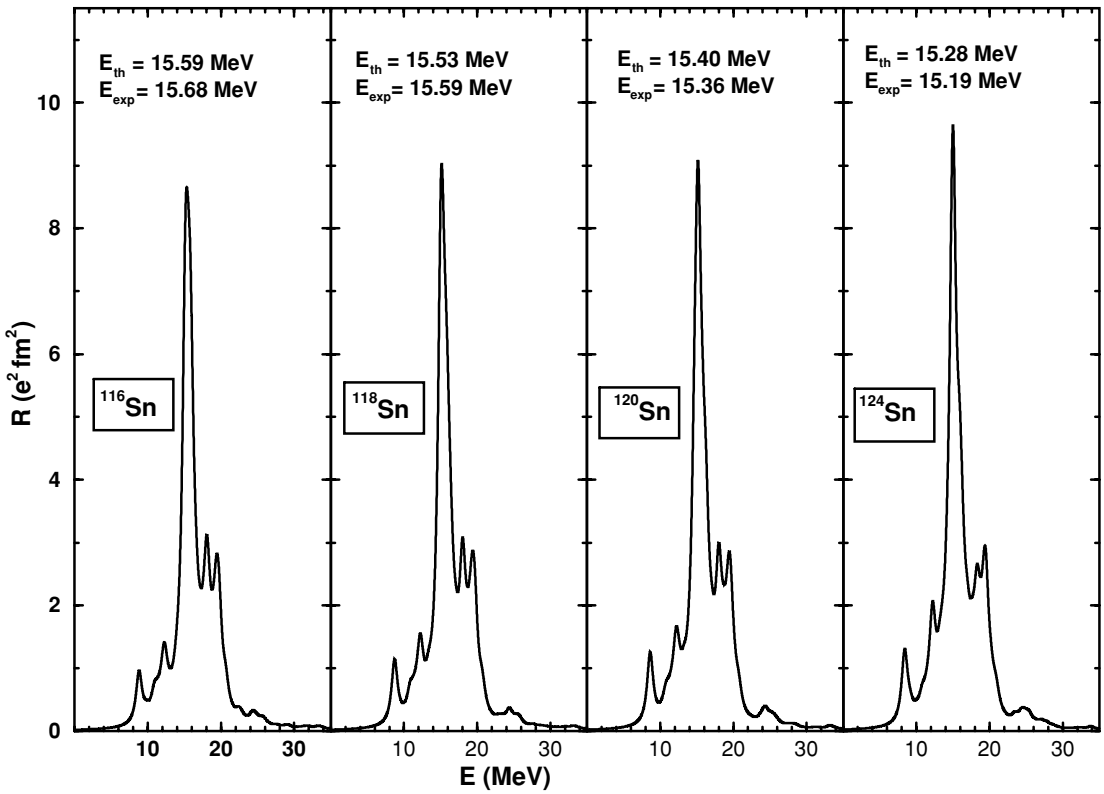

FIG. 4. The RHB+RQRPA isovector dipole strength distributions in ^{116,118,120,124}Sn. The experimental IVGDR excitation energies for the Sn isotopes are compared with the RHB+RQRPA results calculated with the DD-ME2 effective interaction.

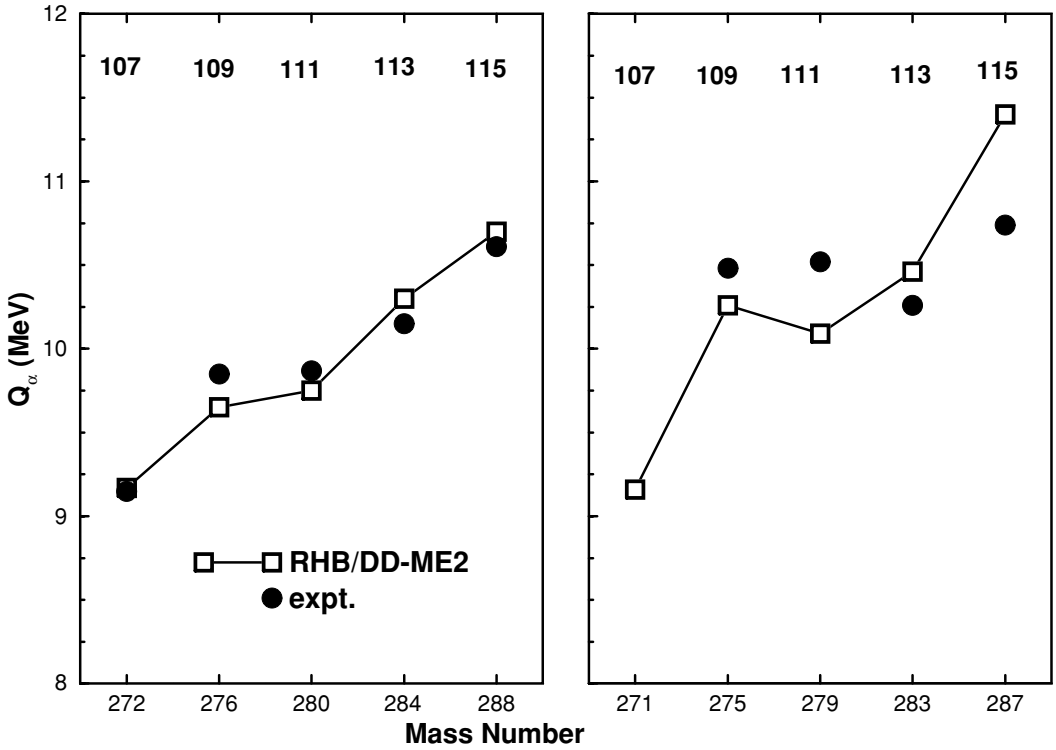

FIG. 5. Theoretical and experimental Q_α values for two α-decay chains starting from the odd-odd nucleus $^{288}115$ and the odd-even nucleus $^{287}115$. The experimental data are from Ref. [39], and the calculated values correspond to transitions between the ground states calculated in the RHB model with the DD-ME2 interaction plus Gogny D1S pairing.

reproduces ground-state properties of superheavies with high accuracy. Of course it is also interesting to analyze predictions for decay chains. In a very recent work [39], evidence has been reported for the synthesis of element $Z = 115$. In Fig. 5 we compare the calculated and experimental Q_α values for two α-decay chains starting from the odd-odd nucleus $^{288}115$ and the odd-even nucleus $^{287}115$. The two superheavy nuclides with $N = 173$ and 172 were produced in the $3n$- and $4n$-evaporation channels following the reaction ^{243}Am + ^{48}Ca [39]. The theoretical Q_α values correspond to transitions between the ground states calculated in the RHB model with the DD-ME2 effective interaction and with the

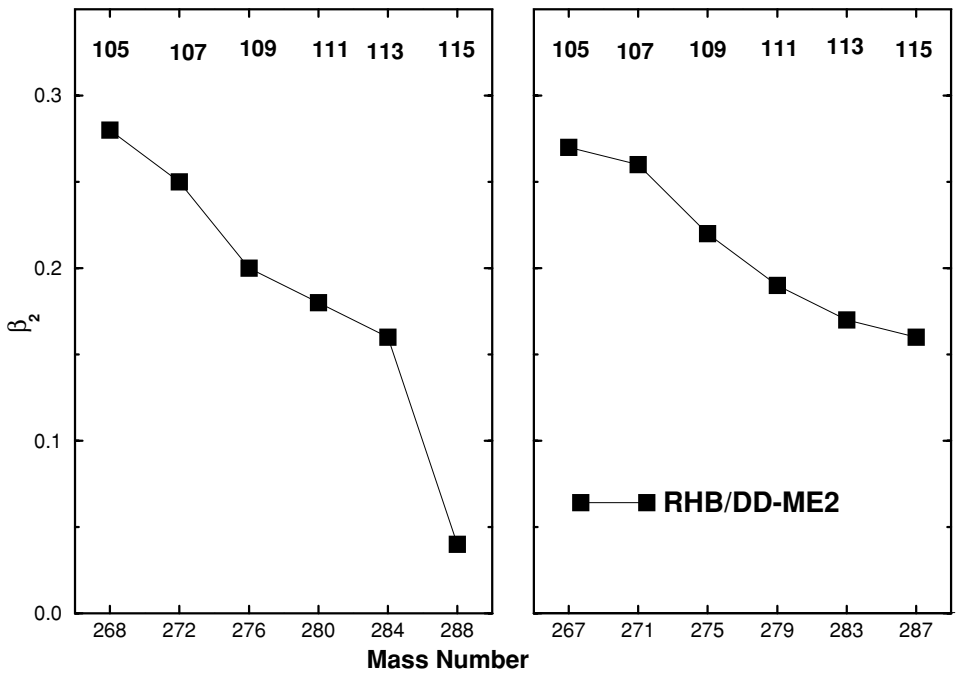

FIG. 6. Calculated ground-state quadrupole deformation parameters β_2 of the superheavy nuclei that belong to the two α-decay chains shown in Fig. 5.

Gogny interaction D1S in the pairing channel. The Dirac-Hartree-Bogoliubov equations and the equations for the meson fields are solved by expanding the nucleon spinors and the meson fields in terms of the eigenfunctions of a deformed axially symmetric oscillator potential. A simple blocking procedure is used in the calculation of odd-proton and/or odd-neutron systems. The blocking calculations are performed without breaking the time-reversal symmetry. We notice that for both α-decay chains the trend of experimental transition energies is accurately reproduced by our calculations. For the odd-odd nucleus $^{288}115$, in particular, the theoretical Q_α values are in excellent agreement with the experimental data. For completeness, in Fig. 6 we also include the ground-state quadrupole deformation parameters β_2 of the superheavy nuclei that belong to the two α-decay chains.

IV. SUMMARY AND CONCLUSIONS

Effective nuclear interactions with density-dependent meson-nucleon vertex functions represent a significant improvement in the relativistic self-consistent mean-field description of the nuclear many-body problem. In a number of recent studies it has been shown that, in comparison with standard nonlinear meson-exchange models, this class of effective interactions provides a more realistic description of asymmetric nuclear matter, neutron matter, and finite nuclei. In particular, these interactions allow for a softer equation of state of nuclear matter (i.e., lower incompressibility) and a lower value of the symmetry energy at saturation.

In this work we have adjusted a new, improved relativistic mean-field effective interaction with explicit density dependence of the meson-nucleon couplings. In comparison with the previous version DD-ME1 that was derived in Ref. [10], the new interaction, denoted DD-ME2, takes into account the results of relativistic RPA analyses [11,12], which provide additional constraints on the parameters that characterize the isoscalar and isovector channels. To illustrate the principal features of the new interaction, we have analyzed ground-state properties and excitation energies of giant resonances. Ground states of spherical and deformed nuclei have been calculated in the RHB model with the DD-ME2 effective interaction in the particle-hole channel, and with the Gogny interaction D1S in the pairing channel. The fully self-consistent RRPA and R(Q)RPA have been used to calculate excitation energies of giant resonances in spherical nuclei. When compared with the results obtained with DD-ME1, the new interaction considerably improves the agreement with experimental data. We particularly emphasize the very good results for the masses of approximately 200 nuclei and for the isoscalar monopole and isovector dipole resonances and the excellent agreement with the recently reported α-decay chains of the new element 115. DD-ME2 represents a valuable addition to the set of relativistic mean-field interactions. Future applications will include the calculation of a microscopic mass table, mapping the drip lines, and a more extensive study of giant resonances.

ACKNOWLEDGMENTS

This work has been supported in part by the Bundesministerium für Bildung und Forschung under Project 06 TM 193, by the Deutsche Forschungsgemeinschaft, and by the Gesellschaft für Schwerionenforschung (GSI) Darmstadt.

[1] M. Bender, P.-H. Heenen, and P.-G. Reinhard, Rev. Mod. Phys. **75**, 121 (2003).
[2] G. A. Lalazissis, P. Ring, and D. Vretenar (Eds.), *Extended Density Functionals in Nuclear Structure Physics*, Lecture Notes in Physics 641 (Springer-Verlag, Berlin/Heidelberg, 2004).
[3] M. Samyn, S. Goriely, P.-H. Heenen, J. M. Pearson, and F. Tondeur, Nucl. Phys. **A700**, 142 (2002).
[4] M. Samyn, S. Goriely, and J. M. Pearson, Nucl. Phys. **A725**, 69 (2003).
[5] S. Goriely, M. Samyn, P.-H. Heenen, J. M. Pearson, and F. Tondeur, Phys. Rev. C **66**, 024326 (2002).
[6] S. Goriely, M. Samyn, M. Bender, and J. M. Pearson, Phys. Rev. C **68**, 054325 (2003).
[7] F. Buchinger, J. M. Pearson, and S. Goriely, Phys. Rev. C **64**, 067303 (2001).
[8] M. V. Stoitsov, J. Dobaczewski, W. Nazarewicz, S. Pittel, and D. J. Dean, Phys. Rev. C **68**, 054312 (2003).
[9] E. Perlinska, S. G. Rohoziński, J. Dobaczewski, and W. Nazarewicz, Phys. Rev. C **69**, 014316 (2004).
[10] T. Nikšić, D. Vretenar, P. Finelli, and P. Ring, Phys. Rev. C **66**, 024306 (2002).
[11] T. Nikšić, D. Vretenar, and P. Ring, Phys. Rev. C **66**, 064302 (2002).
[12] D. Vretenar, T. Nikšić, and P. Ring, Phys. Rev. C **68**, 024310 (2003).
[13] F. Hofmann, C. M. Keil, and H. Lenske, Phys. Rev. C **64**, 034314 (2001).
[14] S. Typel and H. H. Wolter, Nucl. Phys. **A656**, 331 (1999).
[15] C. Fuchs, H. Lenske, and H. H. Wolter, Phys. Rev. C **52**, 3043 (1995).
[16] F. de Jong and H. Lenske, Phys. Rev. C **57**, 3099 (1998).
[17] G. Audi, A. H. Wapstra, and C. Thibault, Nucl. Phys. **A729**, 337 (2003).
[18] A. Krasznahorkay *et al*., Phys. Rev. Lett. **82**, 3216 (1999).
[19] E. G. Nadjakov, K. P. Marinova, and Yu. P. Gangrsky, At. Data Nucl. Data Tables **56**, 133 (1994).
[20] J. F. Berger, M. Girod, and D. Gogny, Comput. Phys. Commun. **63**, 365 (1991).
[21] T. Nikšić, D. Vretenar, G. A. Lalazissis, and P. Ring, Phys. Rev. C **69**, 047301 (2004).
[22] N. Paar, T. Nikšić, D. Vretenar, and P. Ring, Phys. Rev. C **69**, 054303 (2004).
[23] J. F. Berger, M. Girod, and D. Gogny, Nucl. Phys. **A428**, 23 (1984).

[24] N. Paar, P. Ring, T. Nikšić, and D. Vretenar, Phys. Rev. C **67**, 034312 (2003).
[25] S. Raman, C. W. Nestor, Jr., P. Tikkanen, At. Data Nucl. Data Tables **78**, 1 (2001).
[26] D. H. Youngblood, H. L. Clark, and Y. W. Lui, Phys. Rev. Lett. **82**, 691 (1999).
[27] J. Ritman *et al*., Phys. Rev. Lett. **70**, 533 (1993).
[28] B. L. Berman and S. C. Fultz, Rev. Mod. Phys. **47**, 713 (1975).
[29] M. Bender, K. Rutz, P.-G. Reinhard, J. A. Maruhn, and W. Greiner, Phys. Rev. C **60**, 034304 (1999).
[30] W. Nazarewicz, M. Bender, S. Cwiok, P. H. Heenen, A. T. Kruppa, P.-G. Reinhard, and T. Vertse, Nucl. Phys. **A701**, 165 (2002).
[31] Z. Ren, Phys. Rev. C **65**, 051304(R) (2002).
[32] Z. Ren, F. Tai, and D.-H. Chen, Phys. Rev. C **66**, 064306 (2002).
[33] M. S. Mehta, B. K. Raj, S. K. Patra, and R. K. Gupta, Phys. Rev. C **66**, 044317 (2002).
[34] Z. Ren, D.-H. Chen, F. Tai, H. Y. Zhang, and W. Q. Shen, Phys. Rev. C **67**, 064302 (2003).
[35] L. S. Geng, H. Toki, and J. Meng, Phys. Rev. C **68**, 061303(R) (2003).
[36] Y. K. Gambhir, A. Bhagwat, M. Gupta, and A. K. Jain, Phys. Rev. C **68**, 044316 (2003).
[37] T. Sil, S. K. Patra, B. K. Sharma, M. Centelles, and X. Viñas, Phys. Rev. C **69**, 044315 (2004).
[38] T. Bürvenich, M. Bender, J. A. Maruhn, and P.-G. Reinhard, Phys. Rev. C **69**, 014307 (2004).
[39] Yu. Ts. Oganessian, V. K. Utyonkoy, Yu. V. Lobanov, F. Sh. Abdullin, A. N. Polyakov, I. V. Shirokovsky, Yu. S. Tsyganov, G. G. Gulbekian, S. L. Bogomolov, A. N. Mezentsev, S. Iliev, V. G. Subbotin, A. M. Sukhov, A. A. Voinov, G. V. Buklanov, K. Subotic, V. I. Zagrebaev, M. G. Itkis, J. B. Patin, K. J. Moody, J. F. Wild, M. A. Stoyer, N. J. Stoyer, D. A. Shaughnessy, J. M. Kenneally, and R. W. Lougheed, Phys. Rev. C **69**, 021601(R) (2004).